XENON100 – Results and Prospects

Marc Schumann
for the XENON100 collaboration
Physik Institut, University of Zurich, Switzerland
E-mail: marc.schumann@physik.uzh.ch

Abstract. The XENON100 Dark Matter experiment, installed in the Laboratory Nazionali del Gran Sasso (LNGS, Italy), is searching for WIMP type Dark Matter particles scattering off a 62 kg liquid xenon target in a dual phase (liquid/gas) time projection chamber. Careful material selection, a novel detector design, and an upgrade of the passive shield, together with capitalizing the self-shielding power of liquid xenon, are crucial in order to achieve a background of less than 0.01 events kg^{-1} keV^{-1} day^{-1} in the fiducial volume. This background, which has been verified experimentally, is lower than in any other dark matter experiment.
The analysis of 11.2 live days of background data taken during a commissioning run in fall 2009 leads to the first science result of XENON100: No events are observed in a pre-defined fiducial volume of 40 kg mass, excluding spin-independent WIMP-nucleon scattering cross sections above 3.4×10^{-44} cm^2 (at 100 GeV/c^2). Below 80 GeV/c^2, this is the most sensitive exclusion limit so far, disfavouring the interpretation of DAMA and CoGeNT being due to spin-independent, elastic interactions of light mass WIMPs.

1. Introduction

Various indirect astronomical observations at all cosmological length scales suggest that the vast majority of the energy content of the Universe is dark, i.e. invisible over the whole electromagnetic spectrum. Precise measurements of the anisotropies in the cosmic microwave background show that only about 4% of the Universe is made from baryonic matter, 21% is Dark Matter, and 74% is Dark Energy [1] . While the nature of the Dark Energy remains speculative, there are strong indications that Dark Matter is made up from heavy, non-relativistic (cold) particles that build large scale cosmological structures. Since no Standard Model particle has the right properties to be the Dark Matter particle, it must be from *new physics* and many experiments aim to find it. A well motivated candidate is the WIMP (Weakly Interacting Massive Particle), a stable particle arising naturally in many theories beyond the Standard Model, such as supersymmetry or theories with extra dimensions [2].

There are three general approaches to search for Dark Matter: The first is to create the particles in high energy collisions. The second is to search for indirect astronomical evidences such as gamma-lines from Dark Matter annihilation. In the following we will focus on the third method, the direct detection of WIMPs scattering off target nuclei in the laboratory.

Because they are neutral, WIMPs are expected to interact with the target nucleus (nuclear recoil interactions) whereas the main background comes from electromagnetic interactions of gammas and electrons with the atomic electrons (electronic recoil interactions). From the assumed WIMP mass and the velocity distribution one expects to measure a steeply falling, featureless nuclear recoil spectrum at energies of a few keV only. The predicted rates are tiny,

much less than one interaction per kg and day of exposure. Therefore, the experiments have to decrease their background as much as possible in order to be sensitive to WIMPs.

2. Mini-Review on Direct Dark Matter Detection

In this section we want to give a very short overview on the current status of the field of direct Dark Matter searches. This can be done by separating the parameter space for spin-independent WIMP-nucleon scattering into two regions of high and low WIMP masses.

At higher WIMP masses (> 20 GeV/c^2), the field is dominated by CDMS-II and XENON100. The CDMS experiment, located in the Soudan mine (USA), measures the ionization and the phonon signal (heat) deposited by particle interactions in ultra-pure germanium crystals at very low temperatures (<50 mK). The ionization/heat ratio is used to discriminate very effectively between signal and background. Imperfect charge collection at the detector surface might mimic valid signal events, however, this problem is solved with an additional cut on the shape of the charge signal, which allows to run the experiment free of background. In the latest analysis of 612 kg×days blind background data, CDMS observed 2 events in the pre-defined WIMP search region [3]. However, with an expected background of 0.9±0.2 events, the likelihood to observe two or more events is 23% and the statistical significance not large enough to consider these events as WIMP signals. The combined limit from all CDMS-II data taken at Soudan excludes spin-independent cross sections of 3.8×10^{-44} cm^2 for 70 GeV/c^2 WIMPs at 90% CL [3].

The EDELWEISS-II experiment also uses germanium bolometers, however, their design of so-called InterDigit electrodes allows fiducialization within the crystals and rejection of surface events. The collaboration has recently published new preliminary results [4] using 322 kg×days effective exposure, leading to a sensitivity of 5×10^{-44} cm^2 for 80 GeV/c^2 WIMPs (90% CL), which is appoaching the CDMS and XENON sensitivities.

XENON100 gives the best limits between ∼15 and 80 GeV/c^2. It is described in greater detail in the following section of this paper.

At very low WIMP masses (in the order of 10 GeV/c^2), the experimental situation is more complicated, see Fig. 1: Since many years, the DAMA/LIBRA Collaboration claims experimental evidence for an annual modulation signal due to Dark Matter particles, caused by the Earth's motion around the Sun. This modulation, observed from 2–6 keV in ultra-pure NaI(Tl) crystals, has reached a statistical significance of almost 9σ [5], however, without any possibility to discriminate signal from background on an event-by-event basis.

CoGeNT is a prototype germanium detector of 330 g mass operated underground at Soudan. It uses p-type point contacts which allow to reach a very low threshold of 0.4 keV (gamma energy), before the detector is limited by electronic noise. The spectrum taken with an exposure

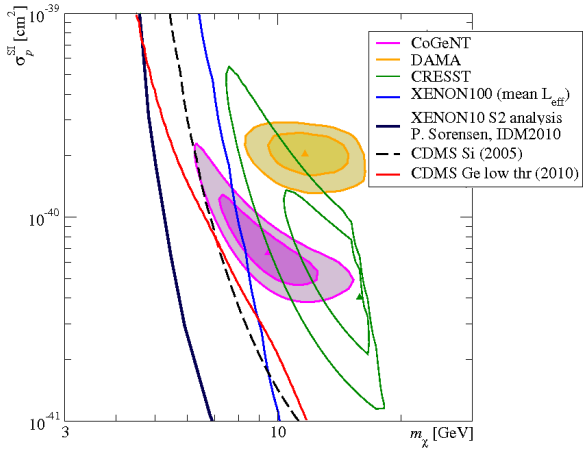

Figure 1. Current experimental situation at low WIMP masses for spin-independent WIMP-nucleon cross sections. The DAMA, CoGeNT, and CRESST-II regions are given at 90% and 3σ CL. The exclusion limits from XENON100, XENON10, and CDMS are 90% CL. Figure reproduced with kind permission from [6].

of 15.5 kg×days rises exponentially at very low energies, a shape which could be explained by a light mass WIMP of ∼10 GeV/c^2. The null-hypothesis, however, has the same χ^2 [7].

The CRESST-II experiment is located at LNGS und uses $CaWO_4$ crystals as target material. The collaboration has recently presented preliminary results [8], observing an excess of nuclear recoils in the oxygen-band which cannot yet be explained by the expected backgrounds. However, the situation and its interpretation remains quite speculative until there is a publication of these results.

Fig. 1 shows the DAMA and CoGeNT results when interpreted as being due to elastic spin-independent WIMP nucleon scattering. They are severely constrained by the non-observation of signals by other experiments: XENON100 (details in Sect. 3) basically excludes DAMA and severly constrains CoGeNT, and a recent re-analysis of CDMS-II data acquired in 2008 with a lowered threshold of 2 keV recoil energy excludes even more parameter space [9].

A preliminary re-analysis of the XENON10 data using the ionization only has been presented recently [10]. While this requires giving up precise information about the position of an interaction as well as signal/background discrimination, it allows to considerably lower the detector threshold for nuclear recoils to about 1 keV. While this analysis sacrifices lots of target mass and does not allow to place competitive results at higher WIMP masses, it provides very strict constraints at low WIMP masses and the DAMA and CoGeNT regions.

3. XENON100

In the remaining sections of this paper, we will focus on the XENON100 experiment and give an outlook into the future.

The XENON collaboration uses liquid xenon (LXe) as target material. Xenon is a heavy target ($A \sim 131$) which enhances the sensitivity for spin-independent WIMP-nucleon scattering. Being an efficient scintillator ($\lambda = 178$ nm), xenon also serves as detector material. Its high density ($\rho \sim 3$ g/cm^3) allows to build compact detectors with excellent self-shielding capabilities. Furthermore, xenon has no long-lived radioactive isotopes, and small admixtures of the radioactive ^{85}Kr can be removed to the ppt level [11].

Liquid xenon detectors provide 3-dimensional interaction vertex reconstruction and signal to background discrimination when operated as a dual-phase (liquid/gas) time projection chamber (TPC), see Fig. 2: An interaction in the LXe generates prompt scintillation light (the S1 signal) and ionizes the target. The ionization electrons are drifted towards the liquid gas interface by a strong electric field. Here, the electrons are extracted into the gas phase and accelerated towards the anode while generating proportional scintillation light (S2). Both signals, S1 and S2, are detected by two arrays of photosensors, one immersed in the liquid for optimal light collection, and one located in the gas phase above the target. The position of the interaction can be reconstructed using the S2 signal distribution on the top array (x, y) and the time difference between prompt S1 and delayed S2 signal (z). Due to their different track densities in the medium, the ratio S2/S1 can be used to discriminate between signal (nuclear recoil interactions) and background (electronic recoils).

XENON100 is the current detector at the 100 kg scale within the phased program of the XENON collaboration. It follows the XENON10 phase which has proven that liquid xenon detectors are able to deliver very competitive results [12]. XENON100 has a total mass of 161 kg of LXe, out of which 62 kg are in the cylindrical target volume which is viewed by two arrays of Hamamatsu R8520 photomultipliers from above (98 PMTs) and below (80 PMTs). The remaining 99 kg of LXe are surrounding the target in 4π. This volume is instrumented with another 64 PMTs and acts as an active veto.

The detector, made from low-radioactivity stainless steel, is enclosed by a passive shield made from 5 cm of ultra-pure OFHC copper, followed by 20 cm of polyethylene, 5 cm of low radioactivity lead, and another 15 cm of standard lead. The whole shield sits on a 20 cm thick

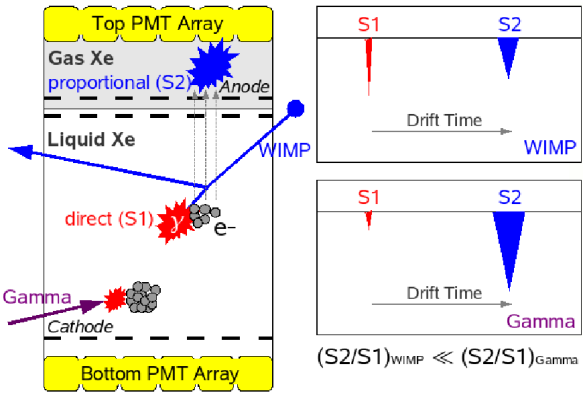

Figure 2. Working principle of a double-phase liquid xenon time projection chamber (TPC): An interaction generates prompt scintillation light (S1) and ionizes the target. The ionization electrons are drifted upwards and extracted into the gas phase where they generate proportional scintillation (S2). The S2 light pattern on the top photosensor array, together with the drift time of the electron cloud, is used to reconstruct the event vertex in (x, y, z). The ratio S2/S1 is different for electronic recoil interactions (background) and nuclear recoil interactions (signal) and is used for discrimination.

slab of polyethylene and is additionally shielded against neutrons with ∼20 cm of water on four sides. All parts with a potentially higher intrinsic radioactivity, such as the pulse tube refrigerator (PTR) to cool the xenon down to −92°C and the feedthroughs, are placed outside the shield.

3.1. Data Analysis and Result

XENON100 is installed underground at Laboratori Nazionali del Gran Sasso (LNGS, Italy) since spring 2008. After extensive calibrations and studies to characterize the detector response, first science data has been taken in fall 2009. This article summarizes the results of this run, which have been published in [13].

Detector Calibration The PMT response is calibrated by stimulating single photoelectron (PE) emission using blue light. The PMT gains were measured regularly and were found to be stable in time within ±2% (σ/μ). The standard gamma line used to obtain the nuclear recoil energy scale from quenching factor measurements (see below) is from ^{57}Co at 122 keV. Since 122 keV gamma rays cannot penetrate deep enough into the detector, the average light yield at this energy was derived to be 2.20(9) PE/keV from calibrations with several gamma lines of higher and lower energy: 40 keV and 80 keV from inelastic neutron scattering processes, 164 keV and 236 keV from neutron activated xenon, and with the higher-energy lines from ^{137}Cs and ^{60}Co.

Because of the geometry of the TPC, the light (S1) and the charge signal (S2) have to be corrected according to their position in the detector. The correction functions have been measured with different sources at various energies, with a mutual agreement of better than 3%. The largest correction for the S2 signal is due to the finite electron lifetime in the LXe: while drifting towards the liquid-gas interface, a certain fraction of ionization electrons is lost to electronegative impurities in the LXe. The charge loss is described by an exponential function with the electron lifetime τ as the main parameter. The data presented here were taken with a maximum lifetime of $\tau \sim 200$ μs.

The drift time of the electrons is used to determine the z-position of the interaction. It is measured with a resolution better than 2 mm, limited by the possibility to separate two independent S2 peaks. For the xy-position, three independent position reconstruction algorithms (neural network, support vector machine, minimal χ^2) yield consistent results for $r < 140$ mm. The precision is better than 3 mm as verified experimentally using a collimated gamma source.

In order to use the $\log_{10}$(S2/S1) parameter to discriminate between electronic and nuclear recoils, the low energy response of the detector to these interactions has to be calibrated.

This has been done using the Compton continuum of ^{60}Co and elastic neutron interactions from an ^{241}AmBe source, respectively. The two populations are well separated and lead to a discrimination of $> 99\%$ at 50% nuclear recoil acceptance.

Background All materials considered for the XENON100 detector and the shield were screened in high purity germanium spectrometers in order to determine their intrinsic radioactivity. Only materials with a reasonable radioactivity were accepted for the detector construction. The detector cavity is constantly purged with boil-off nitrogen in order to avoid radon penetrating the shield. All measured radioactivity values are used as input parameters for a detailed Monte Carlo model of the detector, and the result of the simulation agrees remarkably well with the measured background spectrum over the full energy range [14].

In a fiducial volume of 30 kg mass, XENON100's background rate in the low energy range is 5.3×10^{-3} events keVee^{-1}kg^{-1}day^{-1} (electron recoil equivalent energy, indicating that the energy scale is based on a ^{57}Co calibration) when the active LXe veto is employed. This is a factor 100 lower than XENON10, thus achieving one of the design goals of XENON100. In fact, XENON100 is currently the experiment with the lowest background level of all running dark matter detectors, more than a factor 100 below any other experiment at low energies.

Below 200 keVee, in the energy range of interest, the XENON100 background is dominated by ^{60}Co mainly from the PMTs and ^{85}Kr. The latter has been removed from the LXe by cryogenic distillation [11], and the remaining concentration in this run has been measured to be around 150 ppt via a delayed coincidence technique. This result is consistent with the value from the comparison of the Monte Carlo spectrum and the data [14].

The nuclear Recoil Energy Scale Based on the cut acceptance and the expected recoil spectrum from WIMPs, the energy region of interest for the first Dark Matter analysis has been chosen from 4–20 PE (S1 signal). This region has to be converted to a nuclear recoil equivalent energy scale (given in keVnr) which takes into account the signal losses for nuclear recoil interactions due to quenching.

The relative scintillation efficiency $\mathcal{L}_{\rm eff}$ of a nuclear recoil interaction of energy $E_{\rm nr}$ is the ratio of the light yield at this energy, LY($E_{\rm nr}$), and the light yield of the 122 keV gamma line from ^{57}Co,

$$\mathcal{L}_{\rm eff}(E_{\rm nr}) = \frac{\mathrm{LY}(E_{\rm nr})}{\mathrm{LY}(E_{\rm ee} = 122\ \mathrm{keV})}.$$

In the presence of an electric field, the right hand side of the equation is modified by a factor S_e/S_n to take into account field quenching. The formula allows the conversion of a light signal (measured relative to 122 keV electron recoil equivalent energy $E_{\rm ee}$) to $E_{\rm nr}$. The typical measurement to determine $\mathcal{L}_{\rm eff}$ is illustrated in Fig. 3: The true elastic energy deposition of a neutron from a monoenergetic neutron beam in a LXe chamber is measured via its scattering angle. At the same time, the scintillation light yield is measured in the LXe which gives access to $\mathcal{L}_{\rm eff}$. For lowest energies, however, the scattering angle θ is close to zero, the energy deposition in the LXe is close to the detection threshold, and the measurement becomes very difficult. Therefore, the results of various groups [15, 16] differ more than expected from the stated error bars, see Fig. 4. For a recent discussion of the systematics of these measurements, see [17].

In order to derive a nuclear recoil energy scale from this data, we have chosen to use all $\mathcal{L}_{\rm eff}$ data from scattering measurements and to employ a statistical approach: The thick line in Fig. 4 is the best fit description of the data which was extrapolated to energies below 5 keVnr using a constant function. This choice was motivated by the flat trends seen in some of the data points. The thinner lines give the upper and lower 90% CL contours, the lower contour was very conservatively extrapolated to zero near 1 keVnr using a logarithmic function. In order to

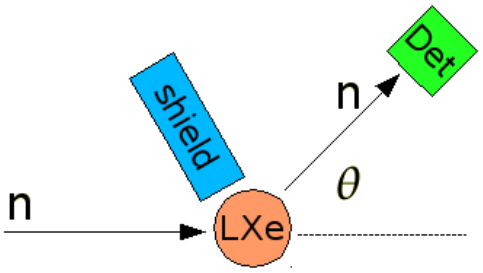

Figure 3. Principle of the measurements of the relative scintillation efficiency $\mathcal{L}_{\rm eff}$: The elastic energy deposition of a monoenergetic neutron beam is measured in a LXe chamber (as S1 light) and via the scattering angle. The observed amount of light relative to the gamma standard ^{57}Co is the relative scintillation efficiency.

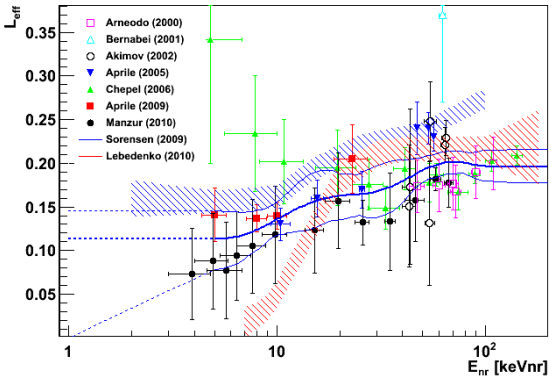

Figure 4. Compilation of all existing $\mathcal{L}_{\rm eff}$ data [15]. The shaded regions are indirect determinations from comparisons of data with simulations [16]. The thick line is the best fit $\mathcal{L}_{\rm eff}$ with a constant extrapolation to lower energies. The thinner lower line is the lower 90% CL contour with a logarithmic extrapolation to zero.

reflect the uncertainty currently present in $\mathcal{L}_{\rm eff}$, we will show the results for both functions, the best fit and the lower 90% CL contour.

In order to clarify this situation, a new measurement of $\mathcal{L}_{\rm eff}$ with improved systematics is currently ongoing at Columbia University. Another independent measurement is in preparation at Zurich University.

Result The data leading to the first XENON100 results were taken in stable conditions in October and November 2009. Altogether 11.2 life days of data have been used for the analysis. The data has not been blinded, however, the analysis has been performed in a quasi-blind way and all cuts and selections were developed on calibration data only.

The WIMP search region between 4 and 20 PE corresponds to 8.7–32.6 keVnr (best fit $\mathcal{L}_{\rm eff}$). The upper bound in $\log_{10}$(S2/S1) space was the median of the nuclear recoil band from the neutron calibration, the lower bound a software threshold of S2 $>$ 300 PE. A simple cylindrical fiducial volume with 40 kg of xenon was chosen for this analysis, and $<$ 0.2 background events were expected in this volume for the given exposure.

Only events with a single S2 peak (single-scatter events) were selected for the WIMP analysis, since the interaction probability of WIMPs is far too small to scatter in the detector twice. Fig. 5 shows the distribution of all single-scatter events in the energy region of interest; the events below the nuclear recoil median are marked in red. No nuclear recoil events are observed in the fiducial volume, indicated in yellow. As expected, the vast majority of the events is located close to the borders of the TPC. Incomplete charge (S2) collection can happen in areas very close to the PTFE walls and the field shaping electrodes of the TPC and is the typical reason for electron recoil events being shifted below the nuclear recoil median. The distribution of the remaining 22 events in the fiducial volume seems to be quite uniform, in agreement with the expectation of a background with a sizeable admixture of ^{85}Kr.

The positions of the events remaining in the fiducial volume in $\log_{10}$(S2/S1) space are shown in Fig. 6. All events are well separated from the WIMP search region. This figure is the most remarkable result of this analysis: It demonstrates that LXe detectors can be indeed used for

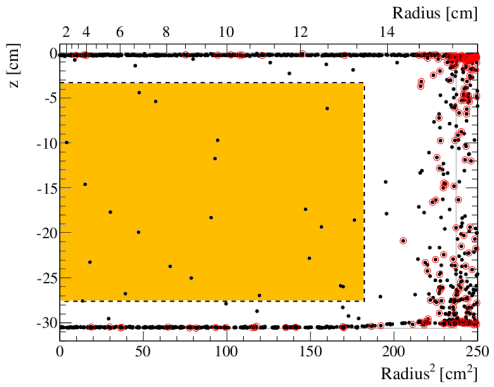

Figure 5. Distribution of the background events in the 11.2 days dataset in the energy region of interest. Most events are close to the edges of the TPC. Only 22 events end up in the fiducial volume of 40 kg mass which is indicated in yellow.

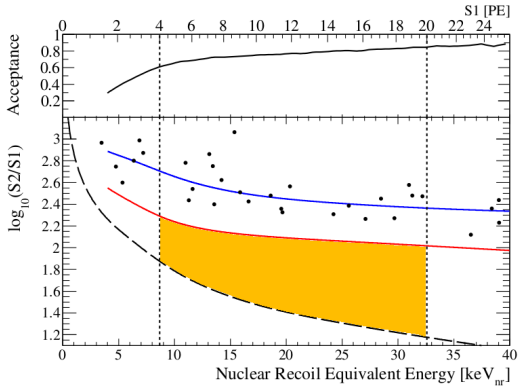

Figure 6. In the $\log_{10}$(S2/S1) space, used for discrimination between signal and background, all remaining events have $\log_{10}$(S2/S1) values well above the nuclear recoil median (red). No event falls in the predefined WIMP search region (yellow).

background-free WIMP searches. The upper part of Fig. 6 gives the energy dependent acceptance function not taking into account the 50% acceptance from $\log_{10}$(S2/S1)-based electronic recoil discrimination.

Poisson fluctuations determine the resolution at the S1 threshold and have to be taken into account to derive a limit from this data in order to treat the resolution properly. Since the expected recoil spectrum from spin-independent WIMP-nucleon scattering is a featureless falling exponential function, the resolution helps to increase the sensitivity at low WIMP masses, as more events from below the threshold fluctuate into signals above the threshold than vice versa. Fig. 7 shows the limits from this analysis, calculated for the two choices of $\mathcal{L}_{\rm eff}$ as discussed above, assuming an isothermal WIMP halo. The acceptance-corrected exposure, weighted by a spectrum of a 100 GeV/c^2 WIMP, is 172 kg×days. For WIMP masses below 80 GeV/c^2, this result places the lowest limit so far. At light WIMP masses, DAMA [5, 18] and CoGeNT [7] are constrained even assuming the conservative $\mathcal{L}_{\rm eff}$.

3.2. Outlook

The previous sections summarized the first Dark Matter results of XENON100, derived from 11.2 life days of data taken during a commissioning run in fall 2009 [13]. In the meantime, about 10× more science data has been acquired and a blind analysis is ongoing. The ultimate sensitivity of XENON100 for spin-independent WIMP-nucleon scattering, based on the background predictions from Monte Carlo simulations, is shown in Fig. 8: For 200 life days exposure and a fiducial volume of 30 kg mass, we expect to reach a sensitivity of $\sigma = 2\times10^{-45}$ cm^2 (at 100 GeV/c^2).

In order to explore the WIMP parameter space down to lower cross sections, or to confirm a possible WIMP detection, we are already in the design phase for XENON1T. This future detector will be a LXe double-phase TPC with a fiducial mass of 1000 kg. Its expected sensitivity to spin-independent WIMP-nucleon cross sections is a few 10^{-47} cm^2 (see Fig. 8). A total amount of about 2.5 tons of xenon will be required for this detector. A large fiducial volume cut, together with careful material selection and LXe purification, will further decrease the background by a factor 100. Detector, LXe handling and purification systems, and shield are currently being designed. Two possible candidates for the light readout are tested: The QUPID [19], a novel

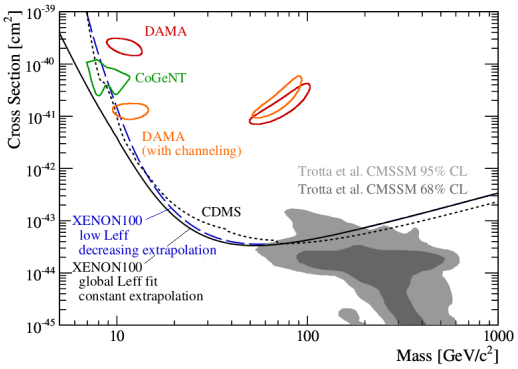

Figure 7. The limit on the spin independent WIMP-nucleon cross section derived from the first XENON100 data. The exclusion plot shows the 90% CL exclusion contours for the two $\mathcal{L}_{\rm eff}$ cases shown in Fig. 4.

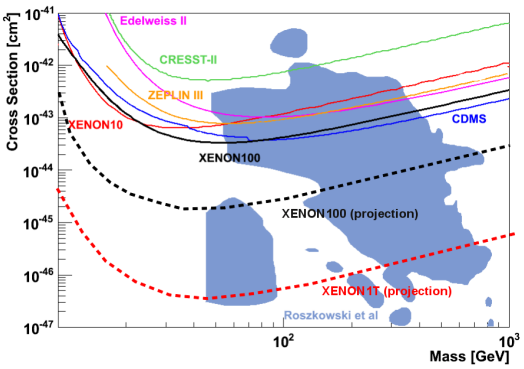

Figure 8. Sensitivity reach of XENON100 and XENON1T for spin independent WIMP-nucleon couplings. XENON1T will be able to explore most of the WIMP parameter space predicted by CMSSM models.

hybrid detector with very low intrinsic background, and the Hamamatsu R11410, a 3" PMT optimized for operation in LXe.

The new DARWIN project [20] aims for the time beyond XENON1T and for cross sections below 10^{-47} cm^2. This design study of a multi-ton Dark Matter detection facility with possibly two targets (xenon/argon) brings together the European groups of the XENON, WARP, and ArDM in one consortium in order to share knowledge and expertise. It is part of the ASPERA roadmap for Astroparticle Physics in Europe.

References

[1] Nakamura K et al. (Particle Data Group) 2010 *J. Phys. G* **37** 075021 and references therein.
[2] Bertone G (ed.) 2010 *Particle Dark Matter* (Cambride: Cambridge University Press)
[3] The CDMS II Collaboration 2010 *Science* **327** 1619
[4] Armengaud R (EDELWEISS-II) 2010 *Preprint* arXiv:1011.2319
[5] Bernabei R et al. (DAMA) 2008 *Eur. Phys. J. C* **56** 333
[6] Schwetz T 2010 *Preprint* arXiv:1011.5432
[7] Aalseth C E et al. (CoGeNT) 2010 *Phys. Rev. Lett.* **106** 131301
[8] Seidel W 2010 *talk presented at IDM2010*
[9] Ahmed Z et al. (CMDS II) 2011 *Phys. Rev. Lett.* **106** 131302
[10] Sorensen P 2010 *talk presented at IDM2010*; Sorensen P et al. (XENON10) 2010 *Preprint* arXiv:1011.6493
[11] Abe K et al. (XMASS) 2009 *Astropart. Phys.* **31** 290
[12] Angle J et al. (XENON10) 2008 *Phys. Rev. Lett.* **100** 021303;
Angle J et al. (XENON10) 2008 *Phys. Rev. Lett.* **101** 091301
[13] Aprile E et al. (XENON100) 2010 *Phys. Rev. Lett.* **105** 131302
[14] Aprile E et al. (XENON100) 2011 *Phys. Rev. D* **83**
[15] Arneodo F et al. 2000 *Nucl. Inst. and Meth. A* **449** 147; Bernabei R et al. 2001 *EPJ direct* **3** 11;
Akimov D et al. 2002 *Phys. Lett. B* **524** 245; Aprile E et al. 2005 *Phys. Rev. D.* **72** 072006;
Chepel V et al. 2006 *Astropart. Phys.* **26** 58; Aprile E et al. 2009 *Phys. Rev. C* **79** 045807;
Manzur A et al. 2010 *Phys. Rev. C* **81** 025808
[16] Sorensen P et al. (XENON10) 2009 *Nucl. Inst. and Meth. A* **601** 339;
Lebedenko V N et al. (ZEPLIN-III) 2009 *Phys. Rev. D* **80** 052010
[17] Manalaysay A 2010 *Preprint* arXiv:1007.3746
[18] Savage C et al. 2009 *J. Cosmol. Astropart. Phys.* **4** 10
[19] Arisaka K et al. 2009 *Astropart. Phys.* **31** 63
[20] Baudis L (DARWIN) 2010 *PoS(IDM2010)***122** *Preprint* arXiv:1012.4764